

# We are IntechOpen, the world's leading publisher of Open Access books Built by scientists, for scientists

6,900

Open access books available

185,000

International authors and editors

200M

Downloads

Our authors are among the

154

Countries delivered to

TOP 1%

most cited scientists

12.2%

Contributors from top 500 universities



WEB OF SCIENCE™

Selection of our books indexed in the Book Citation Index  
in Web of Science™ Core Collection (BKCI)

Interested in publishing with us?  
Contact [book.department@intechopen.com](mailto:book.department@intechopen.com)

Numbers displayed above are based on latest data collected.  
For more information visit [www.intechopen.com](http://www.intechopen.com)



# Chemical Synthesis and Characterization of Luminescent Iron Oxide Nanoparticles and Their Biomedical Applications

*Martin Onani, Leandre Brandt and Zuraan Paulsen*

## Abstract

The syntheses and characterizations of biocompatible luminescent magnetic iron oxide nanoparticles has drawn particular attention as diagnostic and drug delivery tools for treatment of cancer and many other diseases. This chapter focuses on the chemical synthetic methods, magnetic and luminescent properties, including the biomedical applications of iron oxide nanomaterials and luminescent magnetic iron oxide-based nanocomposite materials. The influences of functionalizing with short ligands such as dopamine and L-cysteine on the magnetic properties of synthesized nanoparticles are described. The chapter contains some data on necessary reagents and protocols for bioconjugation aimed at cell culture and step by step the MTT assays used to evaluate cytotoxicity are also presented. In the final section of the chapter, we focus on the biomedical applications specifically for diagnosis and treatment of breast cancer treatment. This chapter also investigates the application of various characterization techniques for analysis of the structural, optical and magnetic properties of the iron oxide nanoparticles and as their nanocomposites.

**Keywords:** nanoparticles, quantum dots, nanocomposite, magnetic, luminescence, biomedical, imaging, cytotoxicity, diagnostics

## 1. Introduction

Over the past few decades, magnetic nanoparticles (MNPs) have attracted tremendous attention due to their unique and tunable chemical and physical properties. Magnetic nanoparticles can selectively target specific biological surfaces of interest owing to the arrangement in dipoles in the absence and presence of an external magnetic field. Iron oxide nanoparticles (IONPs) are one of the mostly used MNPs since they are nontoxic and biodegradable, being promising candidates for use in biology and medicine for example imaging [1, 2], siRNA and drug delivery [3, 4], cell tracking [5], magnetic separation [6, 7] hyperthermia [8, 9], and bio- and chemo-sensing and [10] biomedical applications. Moreover, IONPs are mostly used as magnetic resonance imaging (MRI) probes to differentiate between normal and cancerous cells for diagnosis [11, 12]. Moreover, magnetic imaging has no practical depth limitation for imaging, however spatial resolution is poor and

multiple imaging is problematic. To improve the versatility and efficiency in numerous technologies, the development of hybrid magnetic nanoparticles combining both fluorescent and magnetic properties are being developed [13–23]. The combination of MRI and fluorescent spectroscopy in one nanocomposite opens up unique multimodal properties to monitor complementary information in biological applications such as in multimodal biological imaging, drug delivery systems and medical diagnostics. Despite many problems related to the synthesis of hybrid magnetic-fluorescent nanoparticles, major advances in recent years have been made in this field. For the synthesis, both physical and chemical techniques have been used for the synthesis of IONPs; still, the chemical approach are easier to control the NPs, such as the co-precipitation, thermal decomposition, hydrothermal synthesis, microemulsion, and sol-gel and polyol methods. Of all these approaches, the chemical approach, particularly co-precipitation method is discussed in Section 2. As  $\text{Fe}_3\text{O}_4$  NPs are the mostly used IONPs, in this section we focus on the chemical synthesis of  $\text{Fe}_3\text{O}_4$  NPs. Also, covered in this section is the synthesis of fluorescent-magnetic nanocomposite material, using InP/ZnSe NPs as fluorophore. The syntheses of fluorescent-magnetic nanoparticles are challenging due to chemical stability and the aggregation of the nanoparticles in solution caused by electron transfer interactions between the particles. The main challenge associated is to overcome the quenching of the luminescence of the fluorophore when it is on the particle surface of the magnetic core. This can be due to the electron and energy transfer between the fluorophore and the magnetic nanoparticles [24–26]. The easiest and most commonly used method to overcome this hurdle is to isolate the magnetic core from the fluorescent molecule. This can be achieved by coating the magnetic nanoparticle with a shell before it is attached to the fluorescent structure or by placing a spacer between the two molecules. These solutions lead to most luminescent magnetic nanoparticles to have a core-shell structure [15]. The shell needs to have specific properties namely: non-toxic or harmful to human tissue, should not cause the body to emit an immune response, to avert or reduce agglomeration and reduce non-specific interactions with proteins, cells and other components of biological media. Hence, Section 3 covers several procedures for the functionalization and formation of the fluorescent-magnetic nanocomposite material to overcome these challenges. In Section 4, the biomedical applications of IONPs including MRI, magnetic hyperthermia, magnetic targeting, and cell tracking, with focus on diagnosis for breast cancer treatment are reviewed.

### 1.1 Purpose of the study

Nanocomposite material with dual or multiple properties have shown extensive potential to improve the performance of current cancer diagnostic tools and/or therapy, for biosensor applications, *in vivo* optical imaging or drug delivery. The aim of this project is to synthesize a nanohybrid material with luminescent and magnetic properties and having low or no toxicity, to be used for biological studies.

In this experiment the synthesis of the multifunctional material will be synthesized via the process seen in **Figure 1**. From the diagram the end product, the nanocomposite material, the QDs are expected to cluster around the MNPs.

In order to synthesize the  $\text{Fe}_3\text{O}_4$ -InP/ZnSe bifunctional nanocomposite material, the luminescent InP/ZnSe nanocrystals were prepared separately from the  $\text{Fe}_3\text{O}_4$  magnetic nanoparticles. Once both the MNPs and QDs nanomaterials are synthesized they are both will be functionalized with a compound containing a thiol group. The MNPs and QDs were functionalized with dimercaptosuccinic acid (DMSA) and mercaptopropionic acid (MPA), respectively. Using thiol chemistry, the QDs will directly combine to the surface of the MNPs (as seen in **Figure 1**).

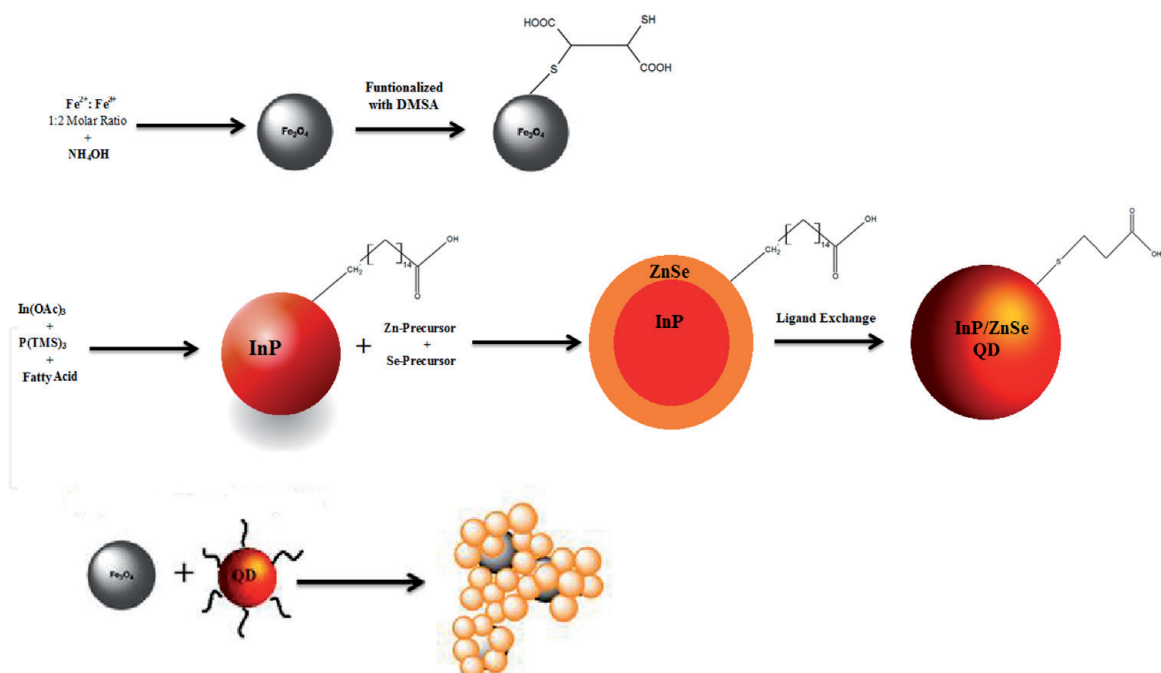


**Figure 1.**  
*Experimental schematic of the synthesis of the magnetic-luminescent nanomaterial.*

## 2. Chemical synthesis of magnetic nanoparticles and magnetic-fluorescent nanoparticles

### 2.1 Magnetic nanoparticles: synthesis

In this chapter, we discuss the general and recent progress of different chemical synthetic pathways for IONPs ( $\text{Fe}_3\text{O}_4$ ). Their small and controllable sizes, easily functionalized, as well as the ability to be manipulated by external magnetic forces [15], are all attractive properties for various applications including biomedical pursuits. The properties of MNPs strongly depended on the synthesis route. Consequently, the controllable synthesis of monodispersed IONPs is critical for controlling their size distribution, structural defects, surface chemistry, and magnetic behavior for application in specific biomedical field. The synthesis of shape-controlled, stable, biocompatible, and monodispersed IONPs have drawn much effort over recent years. IONPs have been produced by various chemical, physical and biological methods which have both advantages and disadvantages (**Table 1**). Chemical synthesis offers significant advantages over other methods, as it is a facile, cost-effective method with ease of control over the NPs characteristics. These methods include thermal decomposition, co-precipitation, microemulsion, hydrothermal synthesis, and sol-gel and polyol methods, also shown in **Table 1** [32]. Of these methods, co-precipitation is the mostly used as it tends to be green, simple and effective with low production cost, high reproducibility and high yields in one synthesis [27]. Hence, it is of interest, and discussed in detail in section below.

#### 2.1.1 Co-precipitation method

Co-precipitation method is the preferred choice among studied synthetic methods for the preparation of  $\text{Fe}_3\text{O}_4$  NPs. It is a simple and classical approach to follow as it is simple, convenient, cheap with high reproducibility, solubility and scalability for large scale production. However, due to the high influence of kinetic factors on the growth of  $\text{Fe}_3\text{O}_4$  NPs, such as low reaction temperatures, this resulted

Techniques	Advantages	Drawbacks
Chemical		
Microemulsion	Precise control over shape and size and high surface area-to-volume ratio	Complex, low yields
Co-precipitation	Simple, convenient, very effective, cheap, standard ambient conditions	Broad size distribution and poor shape control
Sonochemical	Easy with narrow size distribution	No control over shape and medium yield
Hydrothermal	Ease of control over size and shape. High efficiency	High pressure and high reaction temperature
Polyol and sol-gel	Facile with precise control over size and their internal structure	Complicated and high pressures
Electrochemical decomposition	Good control over particle size	Very low reproducibility, rough and amorphous impurities final product
Thermal decomposition	Monodispersed NPs, excellent shape and size control	Only dissolves in non-polar solvents
Physical		
Electron beam lithography	Good control over inter-particle spacing	Costly and use extremely complex apparatus
Gas phase deposition	Easy	Poor control over size
Aerosol	Relatively narrow size range	Complex
Biological		
Bacteria-mediated	Cheap, good reproducibility and scalability, and high yields	Tedious, laborious

*Data edited from [27–31].*

**Table 1.**  
*A comparison of the several synthetic methods of IONPs with advantages and disadvantages.*

in formation of irregularly shaped NPs with broad size distribution. This is the best method for the synthesis of water soluble magnetic nanoparticles. However, it has major drawbacks of broad particle size distribution [27, 33]. In 1982, Rene Massart prepared the first superparamagnetic iron oxide NPs, magnetite ( $\text{Fe}_3\text{O}_4$ ), [17] via an alkaline precipitation of  $\text{FeCl}_3$  and  $\text{FeCl}_2$  mixture in a molar ratio of 1:2 [17]. The NPs were some-like spherical shaped, with diameter in broad size range around 8 nm. Hence, a size selection process using NaCl as an extra electrolyte was used to selectively decrease the electrostatic repulsions between NPs. This caused aggregation and formation of larger colloidal particles in the supernatant with a diameter of about 7 nm [18]. Hence,  $\text{O}_2$ -bearing atmospheres is required for subsequent reactions to form maghemite ( $\text{Fe}_2\text{O}_3$ ) or ferric hydroxide ( $\text{Fe}(\text{OH})_3$ ) [27, 30, 31], due to the sensitivity and instability of magnetite as it is prone to oxidation [34]. In most cases, the co-precipitation method involves some form of mixing  $\text{Fe}^{2+}/\text{Fe}^{3+}$  salt solutions in an alkaline medium at standard or elevated temperatures under inert ( $\text{N}_2$  or Ar) atmospheres to avoid the possible oxidation of  $\text{Fe}^{2+}$  into  $\text{Fe}^{3+}$  [35]. Most papers apply temperatures between 60 and 80°C, some at even higher temperatures [36]. The alkaline solutions commonly used are sodium hydroxide, potassium hydroxide and ammonium hydroxide. The co-precipitation method consists of two major steps—the first is the occurrence of a short nucleation burst at critical supersaturation is reached, and the second involves the slow nucleation growth via diffusion of the solute to the nanocrystal [15]. To obtain monodispersed  $\text{Fe}_3\text{O}_4$  NPs, these two

stages must be kept separate and the  $\text{Fe}^{2+}/\text{Fe}^{3+}$  must be fixed at 1:2 molar ratio. Large amounts of monodispersed IONPs can be easily synthesized by changing certain reaction parameters for example the pH, temperature, ionic strength, composition of iron salts, ratio of ferrous to ferric iron and the type of the base and salt precursors [27]. Depending on the parameters, the particle size can be tuned in size range of 2–15 nm [27] with superparamagnetic properties. In most cases, the particle size increase as reaction time and temperature increase, the faster reaction rate results in formation of monomeric generation of NPs. Moreover, the pH value has shown an important role in controlling the size and stability [16]. Studies have shown that the pH must be kept in the range of 8–14 for monodispersed IONPs. A decrease in the pH value results in the decrease of the diameter or dissolution of the NPs, while increase in pH value show NP tendency to oxidate.

This can be prevented by using a surfactant on the surface of  $\text{Fe}_3\text{O}_4$  NPs which cause repulsive force between radical ions. In addition, the surfactant not only protects the surface of  $\text{Fe}_3\text{O}_4$  NPs, but can also control the size of NPs. In a paper Gao et al. synthesized  $\text{Fe}_3\text{O}_4$  NPs using an aqueous solution of  $\text{FeSO}_4 \cdot 4\text{H}_2\text{O}$ ,  $\text{NaNO}_3$ ,  $\text{NaOH}$ , and citrate as the surfactant [19]. The diameter range was tuned from 20 to 40 nm by changing  $\text{Fe}^{2+}$  concentration. In another paper, Kumar et al. report on an environmentally benign, non-toxic and cost-effective method for the successful synthesis of spherical shaped  $\text{Fe}_3\text{O}_4$  NPs.

Blackberry leaf (ABL) extract is used as capping agent, and added to a solution of  $\text{FeSO}_4 \cdot 7\text{H}_2\text{O}$ , using  $\text{NaOH}$  to adjust the pH to 10–11, the solution was gradually heated between 75 and 80°C. The obtained  $\text{Fe}_3\text{O}_4$  NPs had a size range of  $54.5 \pm 24.6$  nm diameter [40]. In our group, Kiplagat et al. synthesized bare and meso-2,3-dimercaptosuccinic acid (DMSA) capped  $\text{Fe}_3\text{O}_4$  (as shown in **Figure 2**). We prepared bare iron oxide nanoparticles following a simple co-precipitation method by dissolving salts of  $\text{Fe}^{3+}$  and  $\text{Fe}^{2+}$  with a molar ratio of 1:2 at the pH of

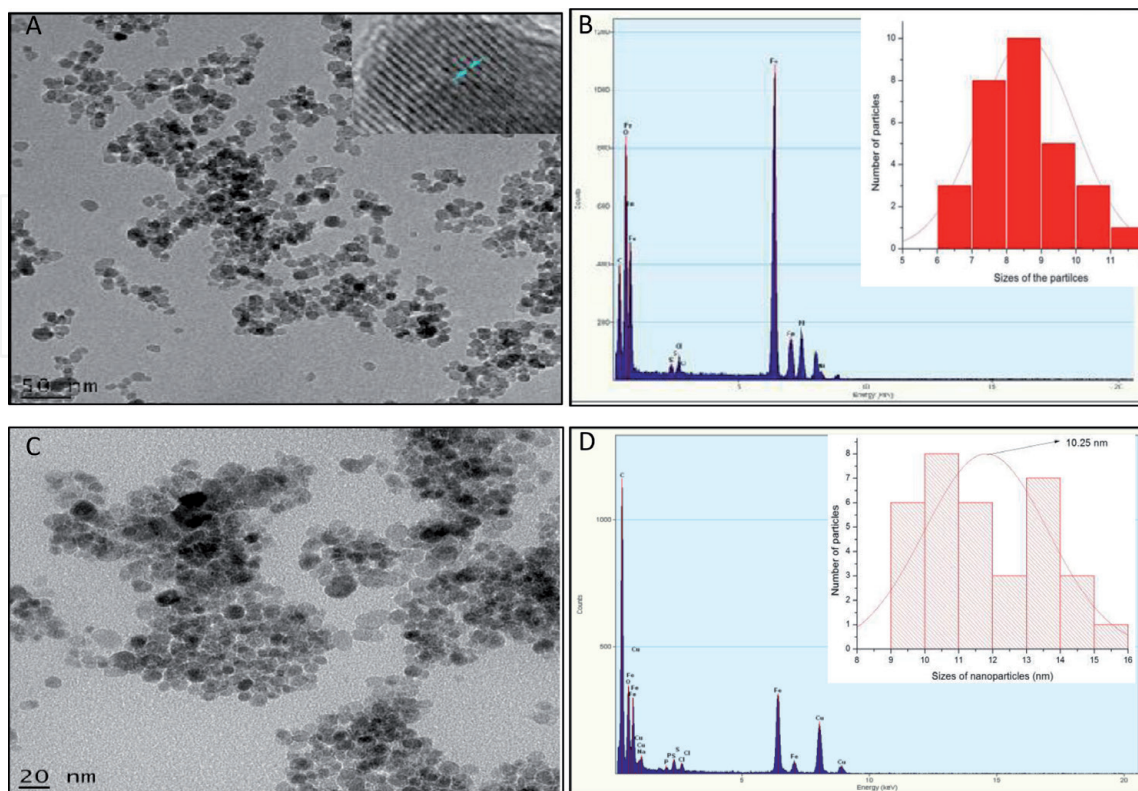


**Figure 2.**  
TEM and EDX of bare and DMSA capped irregularly spherical shaped  $\text{Fe}_3\text{O}_4$  nanoparticles synthesized by co-precipitation method (insets: histograms showing size distribution).

12 in ultra-pure water at 50°C [41]. The DMSA capped iron oxide nanoparticles were prepared by dispersing IONPs in toluene and dimethylsulfoxide solution. The diameter of the bare IONPs range from 6 to 13 nm and the average size of 8.5 nm, whereas the DMSA capped IONPs size distribution range from 9 to 16 nm with an average diameter of 10.25 nm as shown histograms in **Figure 2**. The average size of DMSA capped iron oxide nanoparticles increased slightly compared to the bare iron oxide nanoparticles. Consequently, in our study we found that the synthesis of highly crystalline and monodispersed  $\text{Fe}_3\text{O}_4$  NPs was not as easy to achieve. The capping of the iron oxide nanoparticles with the DMSA resulted to partial agglomeration as seen **Figure 2(a)** and **(c)**. We speculate that the presence of two thiol functional groups in DMSA lead to coupling the nanoparticles, thus the tendency to agglomerate. Similar observations were made by Kumar et al. [40] where they noted that functionalization with ABL led to partial aggregation and broader particle size distribution of IONPs. The use of suitable capping ligands is a widely used to improve their biocompatibility and stability [27, 44], however various approaches are being employed to avoid aggregation of these magnetic nanoparticles that restricts their applications.

In **Figure 3**, we show the XRD patterns of bare and DMSA capped iron oxide nanoparticles. The XRD pattern was matched with JCPDS no. 00-039-1346 and 00-019-0629 for maghemite ( $\alpha\text{-Fe}_2\text{O}_3$ ) and magnetite ( $\text{Fe}_3\text{O}_4$ ), respectively. Our iron oxide nanoparticles were found to be maghemite. This might be due to the IONPS tendency to undergo oxidation as mentioned earlier [27, 30, 31, 35, 36]. A comparison chart of different coated IONPs and nanocomposites, including their characteristics such as the capping agent, physicochemical and magnetometric properties are shown in **Table 2**. The main of objective was to provide a facile method of preparing  $\text{Fe}_3\text{O}_4$  NPs and its corresponding nanocomposites, to overcome the drawbacks of the prior research, particularly a process with less chemical reagents, carried out at standard reaction conditions.

## 2.2 Fluorescent QDs: synthesis

On the other hand, another class of nanomaterials is quantum dots. Quantum dots (QDs) are inorganic fluorescent semiconductor nanoparticles with dimensions in the range of 1–10 nm. The QDs are usually composed of atoms from groups II–VI, III–V, or IV–VI [45]. The nanometer dimensions of the QDs causes a confinement of electron and hole carriers at dimensions smaller than the bulk Bohr excitation radius; this causes phenomenon, called quantum confinement, to occur in these

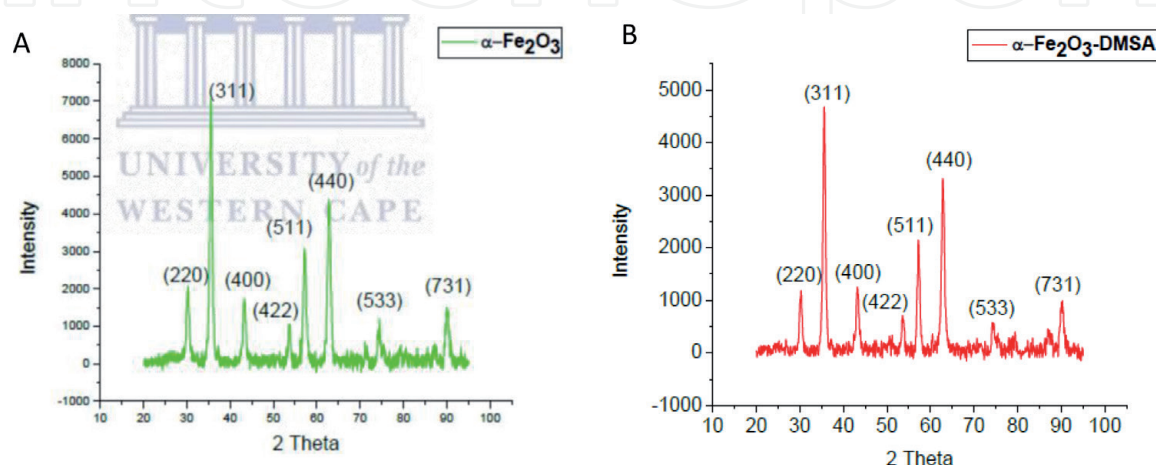


**Figure 3.**  
XRD pattern for bare and DMSA capped iron oxide nanoparticles.

Type of IONPs	Synthetic method	Coating	Physicochemical properties	Magnetometric properties (SQUID)	Application	Reference
MnFe <sub>2</sub> O <sub>4</sub>	Thermal decomposition	1,2-Hexadecanediol, dodecanoic acid, dodecylamine	Spherical shape; 12 nm	M <sub>s</sub> = 298 K, T <sub>b</sub> = 43.2 emu/g (SQUID)	Multimode imaging probes	Lim et al. [26]
Fe <sub>3</sub> O <sub>4</sub>	Thermal decomposition of iron oleate in NaCl	Oleic acid	Octapodes; 20–30 nm	M <sub>s</sub> = 51–71 emu/g, T <sub>b</sub> = 240–290 K (SQUID)	Magnetic resonance imaging	Zhao et al. [37]
Fe <sub>3</sub> O <sub>4</sub>	Co-precipitation	DMSA	Nearly spherical, 1.4–6.5 nm	M <sub>s</sub> = 51.7 emu/g, T <sub>b</sub> = 298 K (VSM)	Lymphoma treatment	Song et al. [38, 39]
Fe <sub>3</sub> O <sub>4</sub>	Green method	Andean blackberry leaf (ABL) extract	Spherical shape, 54.5 ± 24.6 nm	N/A	Degradation of organic dyes, antioxidant	Kumar et al. [40]
Fe <sub>3</sub> O <sub>4</sub>	Co-precipitation	DMSA	Spherical shape, 9–16 nm	M <sub>s</sub> = 43.2 emu/g (SQUID)	Breast cancer treatment	Kiplagat et al. [41]
InP-Fe <sub>3</sub> O <sub>4</sub>	Co-precipitation	DMSA	Agglomerated, unable to obtain particles	M <sub>s</sub> = 6.03 emu/g (SQUID)	Breast cancer treatment	Kiplagat et al. [41]
Core-shell Fe <sub>3</sub> O <sub>4</sub> @SiO <sub>2</sub> @Au	Thermal decomposition, sol-gel and oil-in-water technique	Cetyltrimethylammonium bromide (CTAB)	Spherical shape, 100–110 nm	M <sub>s</sub> = 50–46 emu/g, T <sub>b</sub> = 298 K (SQUID)	Photoacoustic and magnetic resonance imaging detection	Monaco et al. [42]
Fe <sub>m</sub> O <sub>n</sub> -SiO <sub>2</sub>	Co-precipitation	Silica	Irregular nanoflakes; 98–101 nm	M <sub>s</sub> = 11 emu g <sup>-1</sup> (VSM)	Cytotoxicity	Toropova et al. [43]
SiO <sub>2</sub> -FemOn	Co-precipitation	Silica	Core-shell structure; 98–101 nm	M <sub>s</sub> = 37.2 emu g <sup>-1</sup> (VSM)	Cytotoxicity	Toropova et al. [43]

*M<sub>s</sub> = saturation magnetization; T<sub>b</sub> = blocking temperature; D<sub>c</sub> = critical size; and H<sub>c</sub> = coercivity field.*

**Table 2.**  
*A comparison of several methods of the organic and inorganic coated IONPs, and their corresponding characteristics.*

nanoparticles. The QDs have tunable energy, optical and electronic properties which are done by either managing the QDs size or composition. QDs may be produced via various methods. These methods include but not limited to colloidal synthesis, plasma synthesis, self-assembly, and electrochemical assembly. However, to be able to tune the QDs to have desired properties and to produce high quality QDs colloidal synthetic methods are the easiest and the most explored. Since there are several different types of QDs in exists, for simplicities sake this study will focus on InP.

A colloidal synthetic approach to manufacture QDs can either be achieved by a heating-up technique or rapid hot injection method. The heating up method is a batch process and is achieved by adding all the desired chemicals to a reaction vessel at relatively low temperatures or at room temperature, followed by rapidly heating the entire reaction up to a desired temperature that allows for crystal growth to occur. Khanna et al. [46] directly synthesized indium phosphide (InP) nanoparticles by heating a solution of indium powder in n-trioctylphosphine (TOP). The reaction was carried out under an argon atmosphere. The raw materials, the reaction time and temperature were varied to determine which reaction conditions would create the finest results. In addition, their research demonstrated that with high temperatures in conclusion with, short reaction times and a low amount of TOP leads to InP nanoparticles with small particle sizes and less impurity. The formation of the InP is caused by the catalytic activity of indium nanoparticles attempting to reduce C-P bonds found in TOP. The synthesis method is considered to be simple, low cost and avoids the use of hazardous and expensive raw materials.

### *2.2.1 Hot-injection method*

To obtain QDs via the rapid hot injection technique, a main reaction is heated to a desired temperature and room temperature precursors are added to the reaction by rapidly being injected into the reaction. The quick addition of the precursors causes the reaction to supersaturate thus allowing for nucleation to occur. The reaction temperature when the cooler precursor is added, the addition of the precursor also causes the reaction to become diluted. The lowered temperature and the lowered concentration of the reaction materials prevent further nucleation, but nanocrystal growth still occurs. The work of Lui and co-workers used a reduction colloidal approach Lui and co-workers [47] were able to synthesize high quality InP NCs. The synthesis required the use of octadecene as a solvent and stearic acid as a capping ligand. These were heated in the presence of indium acetate, under an inert atmosphere for 30 min. After being heated a  $\text{PCl}_3$ -precursor was added to the solution at  $40^\circ\text{C}$ . The temperature was then elevated to allow the growth of the InP core. By varying the reaction time and the temperature the study showed how the NC growth could be tuned to a desired size and size distribution. Upon further investigation it was demonstrated that, using a HF post-production treatment, the photoluminescence could be vastly enhanced. The research conducted confirms that InP NCs can be synthesized without the use of the hazardous and expensive material  $\text{P}(\text{TMS})_3$ .

## **2.3 Synthesis of IONPs/QD hybrid nanocomposite**

Creating a complex system like this presents a few complications. The fabrication of such a system would require several synthesis and purifications steps, which is time consuming and expensive. Also having a magnetic element in the presence of a fluorescent compound reduces the photoluminescence and could quench the fluorophore [47–50]. There is currently very little information for possible alternatives to the first problem; the second is usually solved by encasing

the MNP's in silica or polymer [24]. In the research conducted by Hong et al. [50], the layer-by-layer (LbL) approach was used to synthesize the magnetic-luminescent nanocomposite. LbL approach is based on the electrostatic attraction of oppositely charged species. In this synthesis, MNPs were used as a template for the multiple deposition of CdTe QDs. The MNPs were synthesized using the co-precipitation of ferric chloride and ferrous chloride. While TGA-capped CdTe QDs were prepared by the addition of  $\text{Cd}^{2+}$  into a solution of NaHTe in the presence of TGA. Using LbL they were able to fabricate  $\text{Fe}_3\text{O}_4/\text{PE}_n/\text{CdTe}$  and  $\text{Fe}_3\text{O}_4(\text{PE}_3/\text{CdTe})_n$  nanocomposite material by varying the number of deposition cycles of polyelectrolyte layers. The polyelectrolyte phases allowed for increased PL intensity while maintaining strong magnetic properties.

The synthesis described by Gua et al. [51], demonstrated the synthesis of a multifunctional system by integrated materials, with luminescent and magnetic properties, into microspheres of quantum dots (QD) with a cross-linked polymer shell. They basically synthesized iron oxide magnetic nanoparticles (MNP) via a co-precipitation method and thiol-capped cadmium telluride (CdTe) by hydrothermal route. The MNP were incorporated into a silica sphere via the Stöber method and the QDs added. These conjugated moieties were capped using a template polymerization. Their technique provides many advantages including the formation of a robust luminescent shell with multicolor bar codes which is generated by the aggregation of the thiol-capped CdTe on the silica particles. The outer shell not only protects the CdTe shells from damage, but also facilitates the covalent bonding of the ligands to the nanoparticles.

The synthesis described by Liu et al. [48], demonstrates the synthesis of a magnetic-luminescent MNP-QD nanocomposite via electrostatic interactions. The two major problems that occur is (i) the close interactions of the QDs and MNPs, when they are embedded in a matrix, material causes photobleaching; (ii) while the layer-by-layer process takes an extremely long time and a lot of effort. In this experiment first CdSe QDs are synthesized via the hydrothermal route. While the MNPs are separately prepared using the co-precipitation of  $\text{Fe}^{2+}$  and  $\text{Fe}^{3+}$  salts, followed by a silica coating by means of the Stöber method, and finally functionalizing the silica coated MNPs with 3-aminopropyltrimethoxysilane (APTS). The final MNPs were added to a solution of CdSe QDs. The new solution was sonicated and stirred for 6 hours at room temperature. The nanocomposite material was collected and separated by magnetic decantation. The luminescent-magnetic nanomaterial was spherical and had a diameter between 95 and 105 nm. The MNP-QD interactions caused a decrease in the PL intensity. The  $M_s$  of the silica-MNPs was  $5.4 \text{ emu g}^{-1}$  and the  $3.8 \text{ emu g}^{-1}$  for the nanocomposite.

The increase attention of multifunctional nanomaterial has led Nai-Qiang et al. [52] to develop a method to synthesize a nanocomposite composed of MNPs and QD material. The synthesis started the QDs and MNPs were prepared separately. The Mn-doped ZnS QDs synthesis began with a solution of  $\text{Zn}(\text{NO}_3)_2$ , manganese acetate and 3-mercaptopropionic acid (MPA) being mixed together. After the mixture undergone a dilution, an adjustment of the pH, and purging the air with  $\text{N}_2$ ,  $\text{NaS}_2$  was injected into the solution. The MNPs were synthesized via the co-precipitation of  $\text{FeCl}_3$  and  $\text{FeSO}_4$ . The MNPs were then coated with  $\text{SiO}_2$  using the Stöber method, finally the coated MNPs were modified with APTS. Using electrostatic interactions, the MNP-QD linkage was able to occur after 6 hours of rapid stirring. The nanocomposite material XRD pattern was a combination of the  $\text{SiO}_2$ -MNP and Mn-doped QD patterns. The TEM results measured the nanocomposite material to be 100–130 nm in size and spherical. The SQUID analysis showed a decrease of from 54 to  $7 \text{ emu g}^{-1}$  once the MNPs were coated with  $\text{SiO}_2$  and the nanocomposite was also roughly  $7 \text{ emu g}^{-1}$ .

Due to the great potential surrounding multifunctional nanomaterial, there is a desire to create a fast, simple and large-scale synthesis of the nanocomposite material. Microwave irradiation (MWI) been successful in synthesizing various nanostructures that Zedan et al. [53] attempted to use the design to develop a novel synthesis of the magnetic-luminescent nanocomposite material. Using microwave synthesis, the  $\text{Fe}_3\text{O}_4$  and CdSe NCs were prepared separately and to create the nanocomposite material a seed-mediated approach was used. The  $\text{Fe}_3\text{O}_4$  NCs were used as seeds and CdSe semiconductor material was allowed to grow around the nanoparticle under MWI. The TEM images of the nanocomposite material confirmed that they maintained the core-shell morphology, were spherical and 10–15 nm in size. The XRD pattern of the nanocomposite material showed the material having good crystallinity. The nanocomposite material maintained the same emission and adsorption peaks as the CdSe QDs. Also changing the irradiation time provides the nanocomposite material with tunable optical properties and the ability to control the luminescent shell's thickness.

As mentioned previously the synthesis of such a material is very complex, Cho et al. [54] tried to optimize the synthesis of MNP-QD hybrid system by using a direct nucleation route. The multifunctional nanomaterial was prepared by first synthesizing the iron oxide NCs via the thermal decomposition of  $\text{FeO}(\text{OH})$  with oleic acid as a surfactant in octadecene. The MNPs which formed were then purified and dispersed in hexane. The synthesis of the complex was created during the synthesis of cadmium selenide (CdSe) QDs via the high temperature decomposition method. Before the nucleation of the CdSe was allowed to take place, a solution of MNPs was injected into the solution, causing the QD to directly bind onto the MNP. The complex was monodispersed, crystalline, with an excitation of 575 nm and emission of 604 nm, and a quantum yield of 5%. The synthesis conditions were then varied in order to optimize the multifunctional nanomaterial produced. By varying the temperatures, injection rate and surfactant composition, created changes in the nanomaterials size, photoluminescence and morphology.

## 2.4 Experimental details

For this study magnetic-luminescent multifunctional nanocomposite material was synthesized. Following the work of Wang et al. [55], the QDs and MNPs were prepared separately. For the  $\text{Fe}_3\text{O}_4$  MNP synthesis the co-precipitation method was chosen. The QDs were synthesized using the rapid hot injection method, we used  $\text{InP}/\text{ZnSe}$  because the study by Brunetti et al. [56] demonstrated that the In-based core-shell QDs are safer for *in vitro* and *in vivo* analysis than Cd-based QDs. The toxicity assessments found that the Cd-based QDs caused cell membrane damaged genetic material and interferes with  $\text{Ca}^{2+}$  homeostasis. The QDs were synthesized using the rapid hot injection technique and then a ligand exchange was performed on them and the resultant QDs were capped with 3-mercaptopropionic acid (MPA). The MNPs were functionalized with meso-2,3-dimercaptosuccinic acid (DMSA). This functionalization was achieved by creating a solution of 30 mM of DMSA in dimethyl sulfoxide (DMSO). This solution was added to a 40 mM of MNPs in toluene, at a 1:1 volume ratio. The resultant solution was stirred until it was observed that a black precipitate was forming. This black precipitate is the newly thiol-capped MNPs. These MNPs were removed from the solution with a magnet, washed with PBS, and dried in an oven. Using thiol chemistry, the QDs will be allowed to bond to the surface of the MNPs. Jeong et al. [57] was able to prepare multifunctional material using a similar synthesis method. The synthesis between the QDs and MNPs was accomplished through a partial ligand exchange reaction.

### 3. Characterization

The synthesized iron oxide magnetic-luminescent nanocomposite, was characterized using high resolution transmission electron microscopy (HR-TEM), photoluminescence (PL), and superconducting quantum interference device (SQUID) analysis.

The multifunctional nanocomposite material was synthesized using a partial ligand exchange. Using the partial ligand exchange method multifunction nanoclusters are formed; this occurred due to using InP/ZnSe in excess. The choice to use excess QDs was an attempt to reduce the quenching of fluoresce quantum dots caused by the MNPs. As seen by the HR-TEM image (**Figure 3**) the use of the InP/ZnSe in large excess compared to a number of MNPs led to enormous particle crowding. This crowding scenario makes it difficult to determine the average size of nanocomposite particles since the quantum dots filled the spaces between the MNPs.

The PL spectrum the MNP-QD nanocomposite confirms that the composite was successfully formed. In this study, it was discovered that in spite of the high ratio of the QDs to MNPs, the black MNPs quenched the fluorescing capability of the QDs, the lowered intensity is observed in the PL spectrum (**Figure 4**). The quenching could be possibly due to energy transfer process resulting from contact between the quantum dots and the surface of the iron oxide particles.

It is also clear that the absorption peak red shifted to 676 nm. This observation was also sufficient evidence for the successful formation of the nanocomposite, as the red shift emission observed in this study is most likely caused by the modification at the surface of the QDs brought by hydrophilic ligands and also immobilization of the MNPs (**Figure 5**).

The nanocomposite material maintained its magnetic properties after the MNPs were conjugated to the QDs as shown by, **Figure 6**, the magnetization curve. Saturation magnetization of  $\text{Fe}_3\text{O}_4$ -InP/ZnSe core-shell nanocomposite  $\sim 5.7$  emu/g. After the MNP's were conjugated to the QD's the saturation magnetization is now a 10% fraction of the original MNPs.

The nanocomposites were exposed to both MCF-12A and KMST 6 cell lines. The cytotoxicity of the nanocomposite is presented in **Figure 7** below.

As shown by the **Figure 7** the cell viability was greater than 90% for all concentrations of the nanocomposite. The findings suggest that the nanocomposites are less toxic.

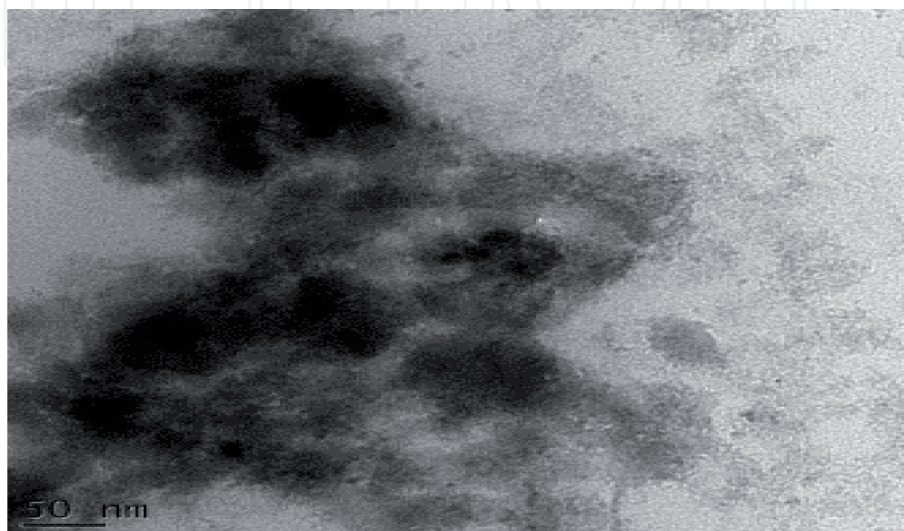


**Figure 4.**  
*MNPs-QDs nanocomposite.*

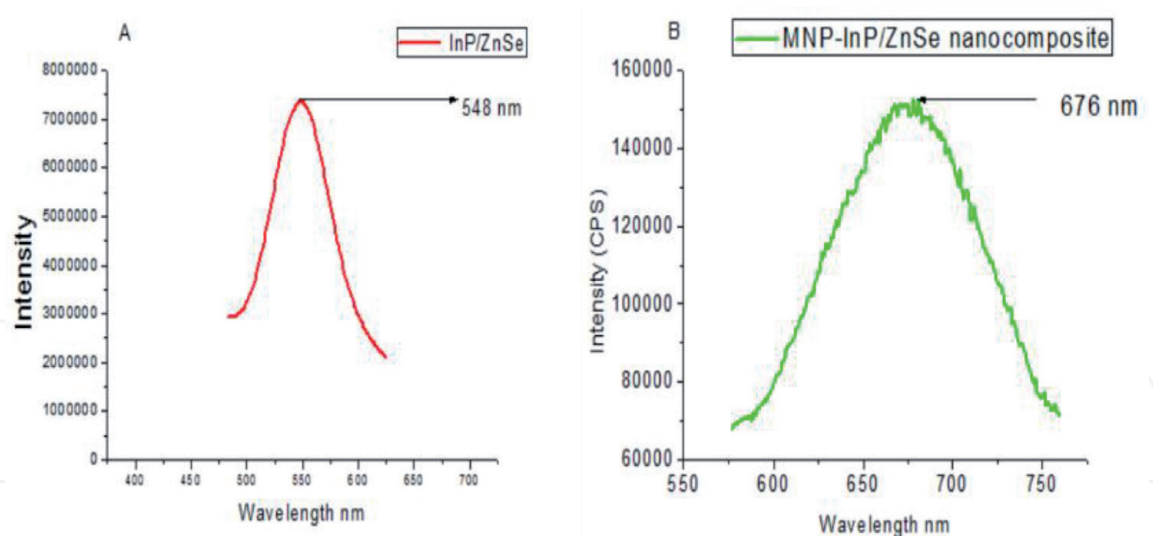


**Figure 5.** PL spectra of InP/ZnSe nanocrystals dispersed in hexane (A) PL spectra of  $\alpha$ -Fe<sub>2</sub>O<sub>3</sub>-InP/ZnSe nanocomposite dispersed in PBS (B) [58].

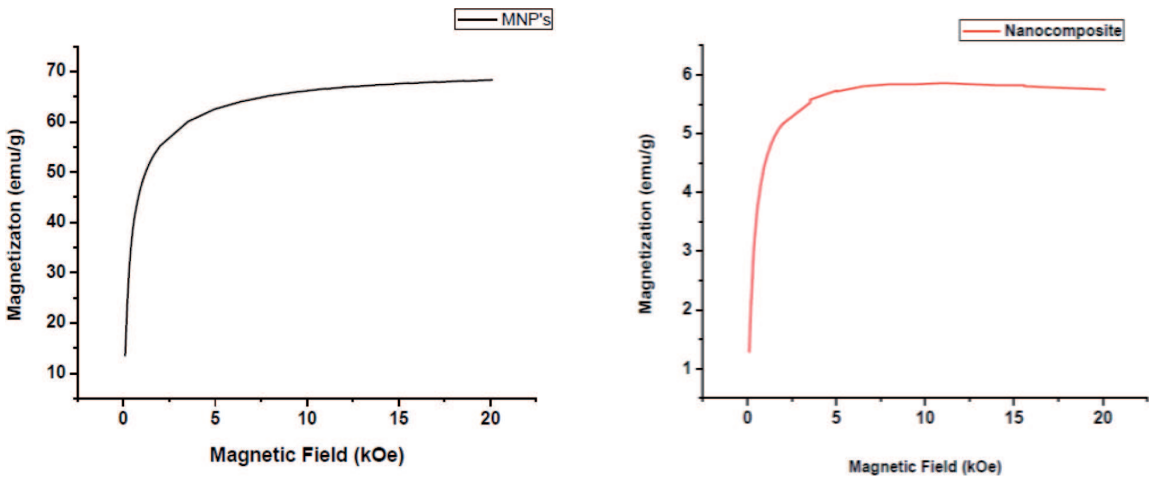


**Figure 6.** Magnetization curves of the MNPs and the nanocomposite material.

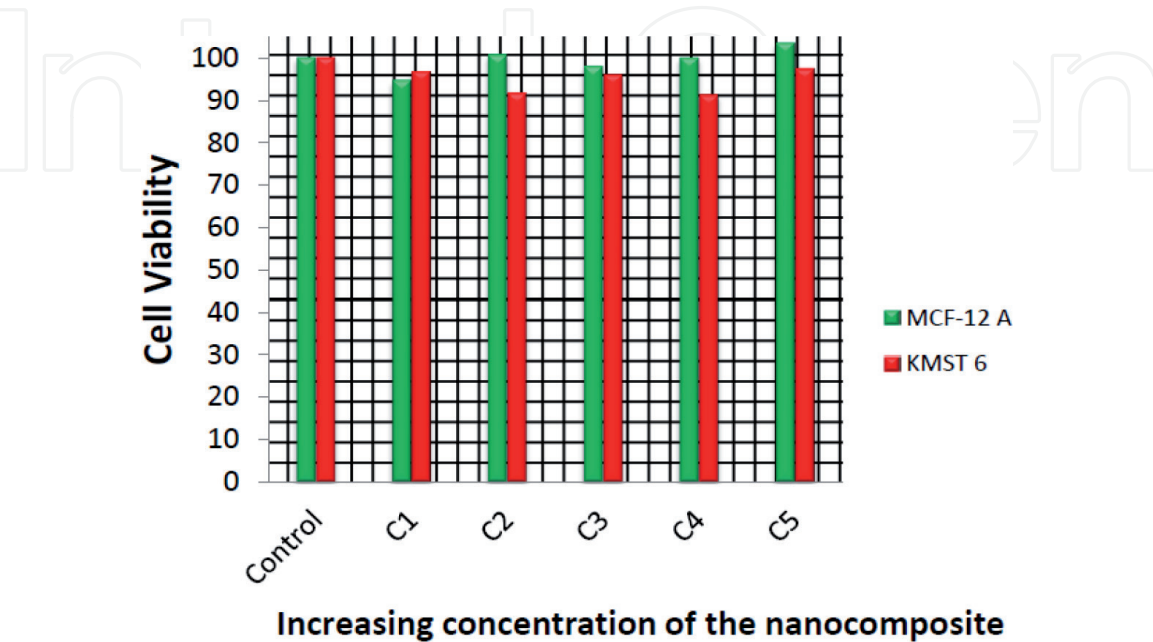


**Figure 7.** Cytotoxicity of the iron oxide-InP/ZnSe nanocomposite [58].

#### **4. Biomedical application of magnetic nanoparticles and fluorescent magnetic nanocomposites**

Increasing attention has been drawn to the synthesis of MNPs for various applications. Magnetic nanomaterials have been observed to possess several distinctive characteristics, these unique capabilities have inspired many ideas in a wide range of biomedical applications [34, 58–68]. These applications include, [34, 63–71], target drug delivery [72], magnetic resonance imaging (MRI) contrasting agent [73, 74], cancer and tumor diagnosis and treatment [75]. Magnetic nanoparticles have demonstrated that they can be manipulated with an external magnetic field and thus to some extent be controlled to successfully reach a specific site of interest in a biological system. It has also been discovered that passing an alternating magnet field over magnetic nanomaterials causes them to heat up; this property makes them very attractive for therapies like hyperthermia, a treatment of cancer that requires selective heating to destroy cancer cells. This property also makes them promising for drug release treatment. Studies have also concluded that superparamagnetic nanoparticles can also improve magnetic resonance imaging (MRI) results. In MRI, aqueous dispersions of superparamagnetic IONPs have shown to be promising contrast agents, since it provides high-resolution images. This characteristic makes it possible to use IONPs as vector in a tracking device for gene and drug delivery. However, most methods require the use of superparamagnetic magnetite with particle size smaller than 20 nm [76]. Over recent years, MNPs have drawn a great deal of interest in cancer treatment, particularly IONPs. Studies have proved that IONPs can easily move into the cells with low cytotoxicity. They possess novel magnetic properties for drug delivery, cell targeting, imaging, tissue engineering and magnetofection. Cancer is known as one of the major causes of death worldwide and survival rates are still significantly low. Great research efforts have been devoted to improving the sensitivity and accuracy of diagnostic treatment for earlier detection and high efficiency, however treatment options not as effective. Recently explored magnetic-fluorescing nanoparticles can be used as simple, efficient and multifunctional diagnostic tool based on MRI [77]. The fluorescent NP emits at certain wavelength appropriate for visual imaging using fluorescence imaging microscopy. The multifunctional nanocomposite will simultaneously allow optical tracking as well as magnetic manipulation of biological processes [78]. Fluorescent-magnetic nanoparticles can be treated as bimodal probes useful for studies of the biological objects using both MRI and fluorescence detection. Bimodal imaging agents serving both for MRI and fluorescence imaging are of special interest. Therefore, we provide a brief introduction on the applications IONPs and fluorescent-IONPs in biomedicine, particularly as contrast agents for MRI diagnosis.

##### **4.1 Applications of IONPs**

IONPs possess unique physicochemical characteristics, as well as superparamagnetic with high surface area, non-toxicity, and biocompatibility [15]. IONPs have effectively been applied in various in biomedical applications [34, 58–68], since they can selectively target a specific biological unit by applying an external magnetic field. Iron oxide nanoparticles of the type,  $\text{Fe}_3\text{O}_4$ , have shown to be promising candidate as a contrast agent for magnetic resonance imaging. This is due to superparamagnetic or paramagnetism which creates an outer magnetic field around itself when exposed to an external magnetic field; this permits the increase of image resolution and decreases aggregation of particles due to fast dephasing of the spins through a so-called magnetic susceptibility effect. This enhances the signal intensity to help distinguish between healthy and unhealthy cells [79–81]. Studies have reported IONPs as promising MRI contrast agents for in vivo rat studies.

In of the studies, rats were anesthetized and subcutaneous injection containing 2.5 mg ( $\text{Fe}_3\text{O}_4$ )/kg body weight of  $\text{Fe}_3\text{O}_4$  samples was given every 6 hours into the right hand of the animal. MRI scans taken after every 6 hours showed accumulation occurred on the lymph nodes, however none was noticed on the left-hand side. The study proved successful imaging of lymphatic system using iron oxide as a contrast agent [82]. At present, numerous studies are still undergoing clinical trials and only two types of dextran-capped IONPs have been clinically approved as MRI contrast agents, highlighted in **Table 3** [83]. These two are commonly known as, Ferucarbotran (Resovist) with particle size of about 60 nm, and Ferumoxides (Feridex in America and Endorem in Europe) have a broader particle size distribution between 120 and 180 nm (**Table 3**) [82, 83].

## 4.2 Application of fluorescent magnetic NPs

Over the years, scientists have shown that one way to improve on current nanomaterials was to combine two or more desired physical properties into one structure. The wish sparked many research ventures into the synthesis or assembly of these type multifunctional materials, also how many entities is effective and which areas could benefit most from these nanocomposites. Incorporation of a fluorescent material within a magnetic NP might modify its band gap energy as well as the luminescence properties [84]. Such multimodal properties are highly desirable specifically in the biomedical diagnosis and therapy [85, 86]. This nanocomposite would not only be improving current applications, but find better ways to achieve a desired outcome. These magnetic-fluorescent nanocomposites could be multimodal assays for in vitro- and in vivo-bioimaging applications such as MRI and fluorescence microscopy [27]. Other exciting applications of these nanocomposites include cell tracking, cytometry and magnetic separation, which could be easily controlled and monitored using fluorescent or confocal microscopy and molecular resonance imaging (MRI) [24, 87, 88]. They could also be used as bimodal agents for cancer therapy, additionally encompassing hyperthermic and photodynamic properties [89]. These fluorescent-magnetic nanocomposites can also be utilized as a multimodal therapeutic and diagnostic tool that can simultaneously locate, diagnose and treat various diseases [90–92]. In another study, Mandal et al. prepared multifunctional nanobiocomposite for targeted drug delivery in cancer therapy. Iron oxide nanoparticle of 15 nm in diameter was used as a contrast agent to enhance MRI and the anticancer drug gemcitabine. In vitro studies between treated and untreated cancer cell lines showed black spots on the gastric cancer cell lines that were treated with the nanobiocomposites whereas no reduction in the signal of the untreated cells. The study concluded that the iron oxide nanobiocomposite can act as contrast agent in MRI and also as a targeted drug delivery system in vivo using rats as an animal model [89]. In similar study, Ahmed et al. prepared the thiol capped-CdTe QDs coated with CTAB. The nanocomposites showed distinct magnetic and fluorescent properties even after isolation with a magnet it still maintained good PL intensity. The nanocomposite was conjugated to antibodies for the imaging of the colon carcinoma cells. No green fluorescence was observed on the surface of the cells. In vitro studies showed low toxicity at 64 fold dilutions. This demonstrated their potential as probes for imaging and ultimately provides a new class of multimodal diagnostics NPs for the complex biological systems [93, 94]. Hence, we focus on the developments of magnetic-fluorescent nanocomposites and their biological applications specifically, multimodal imaging for breast cancer diagnostics.

### 4.2.1 Multimodal bioimaging

Biological imaging or bioimaging is defined as the study of biological processes at the cellular and/or and subcellular level. Several biological imaging techniques

Names	Company	Applications	Relaxometric properties	Coating agent	Hydrodynamic size (nm)
Clariscan ferristene	GE Healthcare	Oral GI imaging	N/A	Sulfonated styrenedivinylbenzene copolymer	3500
Ferumoxsil AMI-121	Guerbet, advanced magnetics	Oral GI imaging	N/A	Silicon	300
Ferumoxides AMI-25	Guerbet, advanced magnetics	Liver imaging, cellular labeling	r1 = 10.1 r2 = 120	Dextran T10	120–180
Lumirem/Gastromark Ferucarbotran SHU-555A	Schering	Liver imaging, cellular labeling	r1 = 9.7 r2 = 189	Carboxydextran	60
Ferumoxytol code 7228	Advanced magnetics	Macrophage imaging blood pool agent, cellular labeling	r1 = 15 r2 = 89	Carboxylmethyldextran	30
Endorem/feridex ferumoxtran-10 AMI-227	Guerbet, advanced magnetics	Metastatic lymph node imaging	r1 = 9.9 r2 = 65	Dextran T10, T1	15–30
Resovist SHU-555C Supravist	Schering	Blood pool agent, cellular labeling	r1 = 10.7 r2 = 38	Carboxydextran	21
Feruglose NC100150	GE Healthcare (discontinue)	Blood pool agent	N/A	PEGylated starch	20
VSOP-C184	Ferropharm	Blood agent, cellular labeling	r1 = 14 r2 = 33.4	Citrate	7

*Data edited from [82].*

**Table 3.**  
*Characteristics of SIONPs agents undergoing clinical investigation clinical or commercial investigation.*

have been developed with different in principles and equipment such as optical bioluminescence, optical fluorescence, ultrasound imaging, MRI, single-photon-emission computed tomography (SPECT), and positron emission tomography (PET), X-ray, thermal imaging, X-ray computed tomography (CT), hyperspectral imaging, and magnetic resonance imaging (MRI) [82]. Over three decades, these techniques have continuously had rapid developments and incremental improvements due to their wide application various biological fields. Multimodal magnetic nanoparticles have significant features as they could act as imaging probes and drug delivery systems. These NPs offer unique characteristic as a dual contrast agent that can combine fluorescent microscopy and MRI. Both techniques are well studied, MRI have been widely applied for in vivo imaging diagnosis, meanwhile fluorescence microscopy are mostly applied for in vitro imaging. Optical imaging is a promising tool as it provides better spatial resolution and performance in sensibility for in vitro imaging, however tissue penetration is limited to few millimeters. Moreover, MRI provides excellent spatial resolution and deep tissue contrast for better in vivo imaging. The amalgamation fluorescent microscopy and MRI opens new possibilities of rapid analysis for diagnosis of diseases and pathogens. In recent years, significant advances have been made in development of fluorescent magnetic nanoparticles as multimodal agents by using magnetic contrast agents. Zhang et al. prepared fluorescent mesoporous silica coated-iron oxide nanoparticles of ~10 nm with high magnetic resonance sensitivity and excellent cell labeling efficiency for detection of neural progenitor cells using MRI [95, 96]. In another study, monodispersed magnetic nanoparticles functionalized with an organic dye showed optical activity and good biocompatibility [93, 94]. In recent study, Guo et al. synthesized superparamagnetic monodispersed core@shell  $\text{CoFe}_2\text{O}_4@\text{MnFe}_2\text{O}_4$  NPs coated with poly(isobutylene-alt-maleic anhydride) PEG and then functionalized with folic acid. The resulting multifunctional

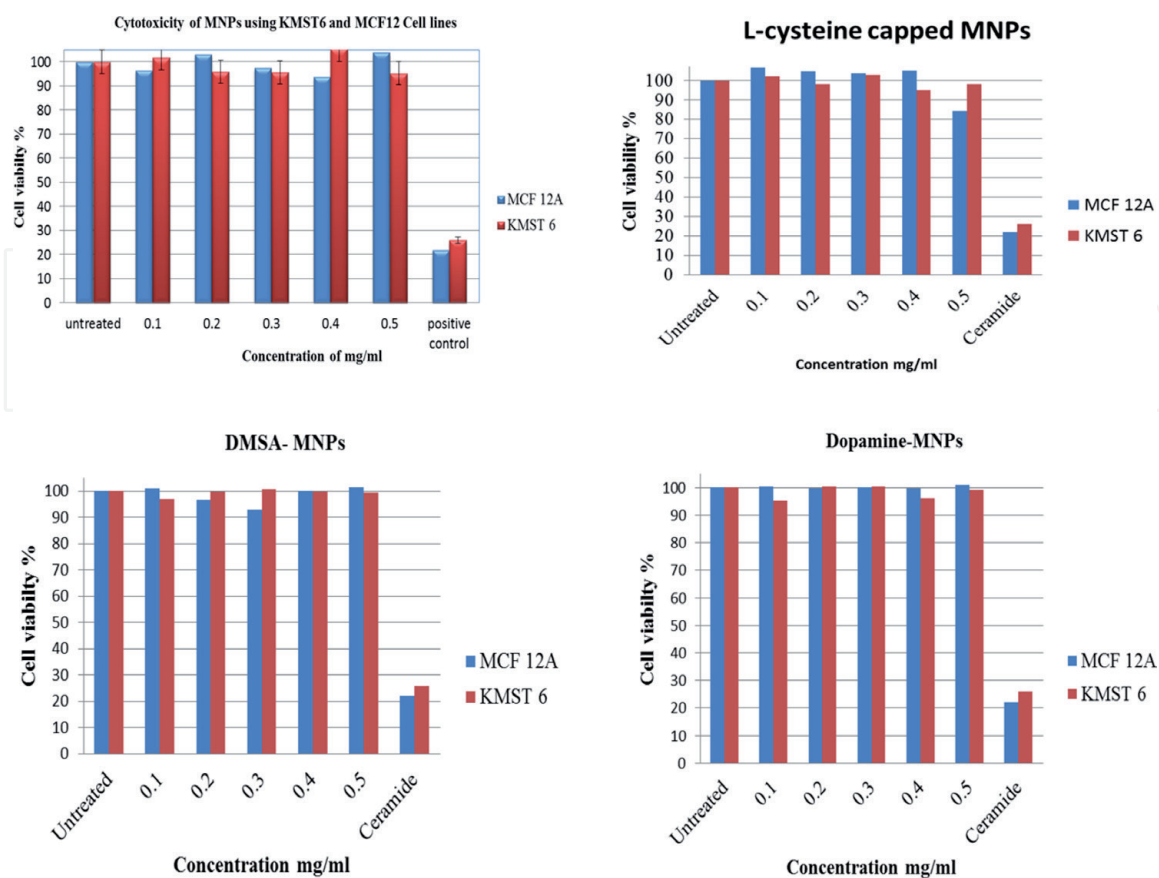


**Figure 8.** Cytotoxicity studies of bare and functionalized iron oxide nanoparticles using MCF-12A and KMST 6 cell lines.

nanocomposite exhibit good biocompatibility, high  $T_2$  relaxation, and long-term fluorescence stability to enhance the targeted MRI and fluorescent tracking for in vivo and in vitro studies [97, 98]. Recent research advancements have produced several excellent magnetic fluorescent nanocomposites. In our study, we prove genes are capable of being used for potential development of serum markers in the diagnosis, of breast cancer or early detection of poor-outcome breast cancer. However, we found that these proteins are present in a very low concentration, which makes the diagnosis a challenging process, however not impossible. The synthesized method used for the preparation of bare and capped iron oxide nanoparticles show low cytotoxicity, which is a strong foundation for future contrast agent for in vivo studies of certain cancer therapies. In addition, it has been proved that different ligand molecules have different effects on the toxicity of the nanoparticles, for example, Liu et al. [93, 94] carried out cytotoxicity study of iron oxide coated with acridine orange using 293 T cells. They varied the concentration of the iron oxide from 0 to 80 mg/mL and observed cell viability greater than 78%. In similar example, In comparison. The lower cell viability observed here could be attributed to acridine orange used and not the iron oxide. In a very recent study, Zhang et al. synthesized superparamagnetic  $Fe_2O_3$  NPs with a diameter of 51.88 nm showed neurotoxic effects in PC12 cell line, in a dose-dependent manner at 60–200 mg/mL, but not at 10–50 mg/mL [99]. The ligands chosen in our study appeared not to affect the toxicity of the iron oxide nanoparticles despite using higher concentration compared to the concentration reported by Liu et al. and Zhang et al. (**Figure 8**) [93, 94, 99].

## 5. Conclusion

We were able to successfully synthesize iron oxide magnetic nanoparticles using the co-precipitation method. The synthesized nanoparticles were then functionalized with DMSA.

We were also able to successfully synthesize InP/ZnSe nanocrystals using the hot injection method. The synthesized nanocrystals were capped with oleic acid, which was the stabilizing agent in the nanocrystals' synthesis. The InP/ZnSe then underwent a ligand exchange and thus the oleic acid capped QDs were replaced with MPA capped QDs.

The ultimate objective of the study was realized when we successfully fabricated a magnetic-luminescent bifunctional nanocomposite material was prepared using thiol-chemistry, this allowed the direct combination of the QDs and MNPs. The nanocomposite material was characterized and observed to exhibit both magnetic and luminescent properties. The SQUID analysis showed that the  $Fe_3O_4$ -InP/ZnSe nanocomposite material has a magnetic saturation of 6.03 emu/g. The PL studies demonstrated that the nanocomposite material had a fluorescence of approximately 40,000 arbitrary units. The nanocomposite material had significantly lower magnetic and fluorescence properties in comparison to their pure forms.

To conclude the study we carried out extensive in vitro cytotoxicity study to evaluate the toxicity of the iron oxide nanoparticles, functionalized iron oxide nanoparticles, InP/ZnSe nanocrystals, and  $Fe_2O_3$ -InP/ZnSe nanocomposite. The KMST 6 and MCF-12A cell lines were exposed to increasing concentration of the nanoparticles. The cells were incubated with the nanoparticles for 24 hours and the cell viability was determined using MTT assay. The cell viability for all types of the nanomaterials was greater than 90% using both MCF-12A and KMST6 cell lines. This suggested that the particles are safe hence not limiting their biological applications and also safe in regard to handling.

IntechOpen

IntechOpen

### **Author details**

Martin Onani\*, Leandre Brandt and Zuraan Paulsen  
Department of Chemistry, University of the Western Cape, Bellville, South Africa

\*Address all correspondence to: monani@uwc.ac.za

### **IntechOpen**

© 2020 The Author(s). Licensee IntechOpen. This chapter is distributed under the terms of the Creative Commons Attribution License (<http://creativecommons.org/licenses/by/3.0>), which permits unrestricted use, distribution, and reproduction in any medium, provided the original work is properly cited. 

## References

- [1] Corot C, Robert P, Idee JM, Port M. Recent advances in iron oxide nanocrystal technology for medical imaging. *Advanced Drug Delivery Reviews*. 2006;**58**:1471-1504
- [2] Sun C, Lee JSH, Zhang M. Magnetic nanoparticles in MR imaging and drug delivery. *Advanced Drug Delivery Reviews*. 2008;**60**:1252-1265
- [3] Veisheh O, Gunn JW, Zhang M. Design and fabrication of magnetic nanoparticles for targeted drug delivery and imaging. *Advanced Drug Delivery Reviews*. 2010;**62**:284-304
- [4] Lee JH, Lee K, Moon SH, Lee YH, Park TG, Cheon J. All-in-one target-cell-specific magnetic nanoparticles for simultaneous molecular imaging and siRNA delivery. *Angewandte Chemie*. 2009;**48**:4174-4179
- [5] Tsai ZT, Wang JF, Kuo HY, Shen CR, Wang JJ, Yen TC. In situ preparation of high relaxivity iron oxide nanoparticles by coating with chitosan: A potential MRI contrast agent useful for cell tracking. *Journal of Magnetism and Magnetic Materials*. 2010;**322**:208-213
- [6] Safarik I, Safarikova M. Magnetic techniques for the isolation and purification of proteins and peptides. *BioMagnetic Research and Technology*. 2004;**2**:7-34
- [7] Zhao Z, Bian Z, Chen L, He X, Wang Y. Synthesis and surface-modifications of iron oxide magnetic nanoparticles and applications on separation and analysis. *Progress in Chemistry*. 2006;**18**:1288-1297
- [8] Ito A, Tanaka K, Honda H, Abe S, Yamaguchi H, Kobayashi T. Complete regression of mouse mammary carcinoma with a size greater than 15 mm by frequent repeated hyperthermia using magnetite nanoparticles. *Journal of Bioscience and Bioengineering*. 2003;**96**:364-369
- [9] Salloum M, Ma R, Zhu L. Enhancement in treatment planning for magnetic nanoparticle hyperthermia: Optimization of the heat absorption pattern. *International Journal of Hyperthermia*. 2009;**25**:309-321
- [10] Kaushik A, Solanki PR, Ansari AA, Malhotra BD, Ahmad S. Iron oxide-chitosan hybrid nanobiocomposite based nucleic acid sensor for pyrethroid detection. *Biochemical Engineering Journal*. 2009;**46**:132-140
- [11] Lacroix LM, Ho D, Sun SH. Magnetic nanoparticles as both imaging probes and therapeutic agents. *Current Topics in Medicinal Chemistry*. 2010;**10**(12):1184-1197
- [12] Lamanna G, Kueny-Stotz M, Mamlouk-Chaouachi H, Ghobril C, Basly B, Bertin A, et al. Dendronized iron oxide nanoparticles for multimodal imaging. *Biomaterials*. 2011;**32**(33):8562-8573
- [13] Kim BH, Lee N, Kim H, An K, Park YI, Choi Y, et al. Large-scale synthesis of uniform and extremely small-sized iron oxide nanoparticles for high-resolution T-1 magnetic resonance imaging contrast agents. *Journal of the American Chemical Society*. 2011;**133**(32):12624-12631
- [14] Ling D, Lee N, Hyeon T. Chemical synthesis and assembly of uniformly sized iron oxide nanoparticles for medical applications. *Accounts of Chemical Research*. 2015;**48**(5):1276-1285
- [15] Sugimoto T. Formation of monodispersed nano- and micro-particles controlled in size, shape, and internal structure. *Chemical Engineering and Technology*. 2003;**26**(3):313-321

- [16] Colombo M, Carregal-Romero S, Casula MF, Gutierrez L, Morales MP, Bohm IB, et al. Biological applications of magnetic nanoparticles. *Chemical Society Reviews*. 2012;**41**(11):4306-4334
- [17] Massart R. Preparation of aqueous magnetic liquids in alkaline and acidic media. *IEEE Transactions on Magnetics*. 1981;**17**(2):1247-1248
- [18] Massart R, Dubois E, Cabuil V, Hasmonay E. Preparation and properties of monodisperse magnetic fluids. *Journal of Magnetism and Magnetic Materials*. 1995;**149**(1-2):1-5
- [19] Hui C, Shen CM, Yang TZ, Bao LH, Tian JF, Ding H, et al. Large-scale  $\text{Fe}_3\text{O}_4$  nanoparticles soluble in water synthesized by a facile method. *Journal of Physical Chemistry C*. 2008;**112**(30):11336-11339
- [20] Chin AB, Yaacob II. Synthesis and characterization of magnetic iron oxide nanoparticles via w/o microemulsion and Massart's procedure. *Journal of Materials Processing Technology*. 2007;**191**(1-3):235-237
- [21] Cai W, Wan JQ. Facile synthesis of superparamagnetic magnetite nanoparticles in liquid polyols. *Journal of Colloid and Interface Science*. 2007;**305**(2):366-370
- [22] Xia T, Wang JP, Wu CL, Meng FC, Shi Z, Lian J, et al. Novel complex-coprecipitation route to form high quality triethanolamine-coated  $\text{Fe}_3\text{O}_4$  nanocrystals: Their high saturation magnetizations and excellent water treatment properties. *CrystEngComm*. 2012;**14**(18):5741-5744
- [23] Xing R, Liu G, Zhu J, Hou Y, Chen X. Functional magnetic nanoparticles for non-viral gene delivery and MR imaging. *Pharmaceutical Research*. 2014;**31**(6):1377-1389
- [24] Corr SA, Rakovich YP, Gun'ko YK. Multifunctional magnetic-fluorescent nanocomposites for biomedical applications. *Nanoscale Research Letters*. 2008;**3**:87-104
- [25] Xu Y, Karmakar A, Wang D, Mahmood MW, Watanabe F, Zhang Y, et al. Multifunctional  $\text{Fe}_3\text{O}_4$  cored magnetic-quantum dot fluorescent nanocomposites for RF nanohyperthermia of cancer cells. *Journal of Physical Chemistry C*. 2010;**114**:5020-5026
- [26] Lim E-K, Yang J, Dinney CPN, Suh J-S, Huh Y-M, Haam S. Self-assembled fluorescent magnetic nanoprobe for multimode-biomedical imaging. *Biomaterials*. 2010;**31**:9310-9319
- [27] Laurent S, Forge D, Port M, Roch A, Robic C, Vander Elst L, et al. *Chemical Reviews*. 2008;**108**:2064-2110
- [28] Ali K, Javed Y, Jamil Y. Size and shape control synthesis of iron oxide-based nanoparticles: Current status and future possibility. In: Sharma SK, editor. *Complex magnetic Nanostructures*. Cham: Springer; 2017. pp. 39-81
- [29] Ali A, Zafar H, Zia M, Ul Haq I, Phull AR, Ali JS, et al. Synthesis, characterization, applications, and challenges of iron oxide nanoparticles. *Nanotechnology, Science and Applications*. 2016;**9**:49-67
- [30] Campos EA, Pinto DVBS, de Oliveira JIS, Mattos ED, Dutra RDL. Synthesis, characterization and applications of iron oxide nanoparticles—A short review. *Journal of Aerospace Technology and Management*. 2015;**7**:267-276
- [31] Wu W, Wu Z, Yu T, Jiang C, Kim WS. Recent progress on magnetic iron oxide nanoparticles: Synthesis, surface functional strategies and biomedical applications. *Science and Technology of Advanced Materials*. 2015;**16**:023501

- [32] Tartaj P, Morales MP, González-Carreño T, Veintemillas-Verdaguer S, Serna CJ. Advances in magnetic nanoparticles for biotechnology applications. *Journal of Magnetism and Magnetic Materials*. 2005;**290-291**:28-34
- [33] Sapsford KE, Algar WR, Berti L, Gemmill KB, Casey BJ, Oh E, et al. Functionalizing nanoparticles with biological molecules: Developing chemistries that facilitate nanotechnology. *Chemical Reviews*. 2013;**113**:1904-2074
- [34] Gupta AK, Gupta M. Synthesis and surface engineering of iron oxide nanoparticles for biomedical applications. *Biomaterials*. 2005;**26**:3995-4021
- [35] Bandhu A, Mukherjee S, Acharya S, Modak S, Brahma SK, Das D, et al. Dynamic magnetic behavior and Mössbauer effect measurements of magnetite nanoparticles prepared by a new technique in the co-precipitation method. *Solid State Communications*. 2009;**149**:1790-1794
- [36] Ozkaya T, Toprak MS, Baykal A, Kavas H, Koseoglu Y, Aktas B. Synthesis of Fe<sub>3</sub>O<sub>4</sub> nanoparticles at 100°C and its magnetic characterization. *Journal of Alloys and Compounds*. 2009;**472**:18-23
- [37] Zhao Z, Zhou Z, Bao J, Wang Z, Hu J, Chi X, et al. Octapod iron oxide nanoparticles as high-performance T<sub>2</sub> contrast agents for magnetic resonance imaging. *Nature Communications*. 2013;**4**:2266. DOI: 10.1038/ncomms3266
- [38] Song L, Zhang W, Chen H, Zhang X, Wu H, Ma M, et al. *International Journal of Nanomedicine*. 2019;**14**:921-936
- [39] Guoa AL, Chenc H, Hea N, Denga Y. Effects of surface modifications on the physicochemical properties of iron oxide nanoparticles and their performance as anticancer drug carriers. *Chinese Chemical Letters*. 2018;**29**(12):1829-1833. DOI: 10.1016/j.cclet.2018.10.038
- [40] Kumar B, Smita K, Cumbal L, Debut A, Galeas S, Guerrero VH. Phytosynthesis and photocatalytic activity of magnetite (Fe<sub>3</sub>O<sub>4</sub>) nanoparticles using the Andean blackberry leaf. *Materials Chemistry and Physics*. 2016;**179**:310-315
- [41] Kiplagat A, Onani MO, Meyer M, Akenga TA, Dejene FB. Synthesis and characterization of luminescence magnetic nanocomposite. *Physica B: Condensed Matter*. 2015:1-9. DOI: 10.1016/j.physb.2015.08.037
- [42] Monaco I, Arena F, Biffi S, Locatelli E, Bortot B, La Cava F, et al. Synthesis of lipophilic core-shell Fe<sub>3</sub>O<sub>4</sub>@SiO<sub>2</sub>@Au nanoparticles and polymeric entrapment into nanomicelles: A novel nanosystem for in vivo active targeting and magnetic resonance-photoacoustic dual imaging. *Bioconjugate Chemistry*. 2017;**28**(5):1382-1390. DOI: 10.1021/acs.bioconjchem.7b00076
- [43] Toropova YG, Golovkin AS, Malashicheva AB, Korolev DV, Gorshkov AN, Gareev KG, et al. In vitro toxicity of Fe<sub>m</sub>O<sub>n</sub>, FemOn-SiO<sub>2</sub> composite, and SiO<sub>2</sub>-FemOn core-shell magnetic nanoparticles. *International Journal of Nanomedicine*. 2017;**12**:593-603. DOI: 10.2147/IJN.S122580
- [44] Kim DK, Mikhaylova M, Zhang Y, Muhammed M. Protective coating of superparamagnetic iron oxide nanoparticles. *Chemistry of Materials*. 2003;**15**:1617-1627
- [45] Xu S, Kumar S, Nann T. Rapid synthesis of high-quality InP nanocrystals. *American Chemical Society*. 2006;**128**:1054-1055
- [46] Khanna PK, Juna K, Honga KB, Baega J, Mehrotra GK. Synthesis of indium phosphide nanoparticles via

catalytic cleavage of phosphorus carbon bond in n-trioctylphosphine by indium. *Materials Chemistry and Physics*. 2005;**92**:54-58

[47] Lui B, Huang W, Wang D, Xie W, Yu M, Yao A. Fabrication of luminescent-superparamagnetic CdSe-QDs/SiO<sub>2</sub>/Fe<sub>3</sub>O<sub>4</sub> nanocomposite particles. *NSIT-Nanotech*. 2008;**2**:297-301

[48] Liu D, Tong L, Shi J, Yang H. Luminescent and magnetic properties of YVO<sub>4</sub>:Ln<sup>3+</sup>@Fe<sub>3</sub>O<sub>4</sub> (Ln<sup>3+</sup>=Eu<sup>3+</sup> or Dy<sup>3+</sup>) nanocomposites. *Journal of Alloys and Compounds*. 2012;**512**:361-365

[49] Liu Z, Kumbhar A, Xu D, Zhang J, Sun Z, Fang J. Coreduction colloidal synthesis of III-V nanocrystals: The case of InP. *Angewandte Chemie International*. 2008;**47**:3540-3542

[50] Hong X, Li J, Wang M, Xu J, Guo W, Li J, et al. Fabrication of magnetic luminescent nanocomposites by a layer-by-layer self-assembly approach. *Chemistry of Materials*. 2004;**16**:4022-4027

[51] Gua J, Yang W, Wang C, He J, Chen J. Poly(N-isopropylacrylamide)-coated luminescent/magnetic silica microspheres: Preparation, characterization, and biomedical applications. *Chemistry of Materials*. 2006;**18**:5554-5562

[52] Nai-Qiang Y, Ling L, Jie-Mei L, Yan-Song L, Mao-Gang G, Yi-Zhi W, et al. Preparation and characterization of nontoxic magnetic-luminescent nanoprobe. *Chinese Physics B*. 2012;**21**(11):116101-116106

[53] Zedan AF, Abdelsayed V, Mohamed MB, Samy E-SM. Rapid synthesis of magnetic/luminescent (Fe<sub>3</sub>O<sub>4</sub>/CdSe) nanocomposites by microwave irradiation. *Journal of Nanoparticle Research*. 2013;**15**:1312

[54] Cho M, Contreras EQ, Lee SS, Jones CJ, Jang W, Colvin VL. Characterization and optimization of the fluorescence of nanoscale iron oxide/quantum dot complexes. *Journal of Physical Chemistry C*. 2014;**118**:14606-14616

[55] Wang D, He J, Rosenzweig N, Rosenzweig Z. Superparamagnetic Fe<sub>2</sub>O<sub>3</sub> beads-CdSe/ZnS quantum dots core-shell nanocomposite particles for cell separation. *Nano Letters*. 2004;**4**(3):409-413

[56] Brunetti V, Chibli H, Fiammengo R, Galeone A, Malvindi MA, Vecchio G, et al. InP/ZnS as a safer alternative to CdSe/ZnS core/shell quantum dots: In vitro and in vivo toxicity assessment. *Nanoscale*. 2012:1-11

[57] Jeong J, Kwon E, Cheong T, Park H, Cho N, Kim W. Synthesis of multifunctional Fe<sub>3</sub>O<sub>4</sub>-CdSe/ZnS nanoclusters coated with lipid a toward dendritic cell-based immunotherapy. *ACS Applied Materials & Interfaces*. 2014;**6**:5297-5307

[58] Ayabei K. Fabrication of luminescent magnetic nanocomposite for diagnosis of breast cancer [A thesis submitted to the Faculty of Natural Sciences]. University of the Western Cape; 2016

[59] Hilger I, Hergt R, Kaiser WA. Use of magnetic nanoparticle heating in the treatment of breast cancer. *IEE Proceedings Nanobiotechnology*. 2005;**152**:33-39

[60] Du K, Zhu YH, Xu HB, Yang XL. Multifunctional magnetic nanoparticles: Synthesis, modification and biomedical applications. *Progress in Chemistry*. 2011;**23**:2287-2298

[61] Huang SH, Juang RS. Biochemical and biomedical applications of multifunctional magnetic nanoparticles: A review. *Journal of Nanoparticle Research*. 2011;**13**:4411-4430

- [62] Schladt TD, Schneider K, Schild H, Tremel W. Synthesis and bio-functionalization of magnetic nanoparticles for medical diagnosis and treatment. *Dalton Transactions*. 2011;**40**:6315-6343
- [63] Mahmoudi M, Serpooshan V, Laurent S. Engineered nanoparticles for biomolecular imaging. *Nanoscale*. 2011;**3**:3007-3026
- [64] Le Trequesser Q, Seznec H, Delville MH. Functionalized nanomaterials: Their use as contrast agents in bioimaging: Mono- and multimodal approaches. *Nanotechnology Reviews*. 2013;**2**:125-169
- [65] Yan K, Li PH, Zhu HE, Zhou YJ, Ding JD, Shen J, et al. Recent advances in multifunctional magnetic nanoparticles and applications to biomedical diagnosis and treatment. *RSC Advances*. 2013;**3**:10598-10618
- [66] Padmanabhan P, Kumar A, Kumar S, Chaudhary RK, Gulyas B. Nanoparticles in practice for molecular-imaging applications: An overview. *Acta Biomaterialia*. 2016;**41**:1-16
- [67] Cherukula K, Lekshmi KM, Uthaman S, Cho K, Cho CS, Park IK. Multifunctional inorganic nanoparticles: Recent progress in thermal therapy and imaging. *Nanomaterials*. 2016;**6**:76
- [68] Nishio K, Ikeda M, Gokon N, Tsubouchi S, Narimatsu H, Mochizuki Y, et al. Preparation of size-controlled (30-100 nm) magnetite nanoparticles for biomedical applications. *Journal of Magnetism and Magnetic Materials*. 2007;**310**:2408-2410
- [69] Jun YW, Lee JH, Cheon J. Chemical design of nanoparticle probes for high-performance magnetic resonance imaging. *Angewandte Chemie, International Edition*. 2008;**47**:5122-5135
- [70] Sudimack JBA, Lee RJ. Targeted drug delivery via the folate receptor. *Advanced Drug Delivery Reviews*. 2000;**41**:147-162
- [71] Hu F, Wei L, Zhou Z, Ran Y, Li Z, Gao M. Preparation of biocompatible magnetite nanocrystals for in vivo magnetic resonance detection of cancer. *Advanced Materials*. 2006;**18**:2553-2556
- [72] Song H, Choi J, Huh Y, Kim S, Jun Y, Suh J, et al. Surface modulation of magnetic nanocrystals in the development of highly efficient magnetic resonance probes for intracellular labeling. *Journal of the American Chemical Society*. 2005;**127**:9992-9993
- [73] Jordan A, Scholz R, Maier-hauff K, Johannsen M, Wust P, Nadobny J, et al. Presentation of a new magnetic field therapy system for the treatment of human solid tumors with magnetic fluid hyperthermia. *Journal of Magnetism and Magnetic Materials*. 2001;**22**:5118-5126
- [74] Sun S, Zeng H. Size-controlled synthesis of magnetite nano-particles. *Journal of the American Chemical Society*. 2002;**124**:8204-8205
- [75] Kalber TL, Smith CJ, Howe FA, Griffiths JR, Ryan AJ, Waterton JC, et al. *Investigative Radiology*. 2005;**40**: 784-791
- [76] Iliuk AB, Hu L, Tao WA. *Analytical Chemistry*. 2011;**83**:4440-4452
- [77] Mascini M, Palchetti I, Tombelli S. *Angewandte Chemie (International Ed. in English)*. 2012;**51**:1316-1332
- [78] Zhang B, Chen B, Wang Y, Guo F, Li Z, Shi D. *Journal of Colloid and Interface Science*. 2011;**353**: 426-432

- [79] Dunn JF, Roche MA, Springett R, et al. Monitoring angiogenesis in brain using steady-state quantification of  $\Delta R_2$  with MION infusion. *Magnetic Resonance in Medicine*. 2004;**51**(1):55-61
- [80] Mandal A, Sekar S, Kanagavel M, Chandrasekaran N, Mukherjee A, Sastry TP. *Biochimica et Biophysica Acta*. 2013;**1830**:4628-4633
- [81] Wang YXJ, Hussain SM, Krestin GP. Superparamagnetic iron oxide contrast agents: Physicochemical characteristics and applications in MR imaging. *European Radiology*. 2001;**11**(11):2319-2331
- [82] Jing LH, Ding K, Kershaw SV, Kempson IM, Rogach AL, Gao MY. Magnetically engineered semiconductor quantum dots as multimodal imaging probes. *Advanced Materials*. 2014;**26**:6367-6386
- [83] Abdullah Mirzaie R, Kamrani F, Anaraki Firooz A, Khodadadi AA. *Materials Chemistry and Physics*. 2012;**133**:311-316
- [84] Kim J, Lee JE, Lee SH, Yu JH, Lee JH, Park TG, et al. *Advanced Materials*. 2008;**20**:478-483
- [85] Lee JE, Lee N, Kim T, Kim J, Hyeon T. *Accounts of Chemical Research*. 2011;**44**:893-902
- [86] Jana NR. Design and development of quantum dots and other nanoparticles based cellular imaging probe. *Physical Chemistry Chemical Physics*. 2011;**13**:385-396
- [87] Koole R, Mulder WJM, van Schooneveld MM, Strijkers GJ, Meijerink A, Nicolay K. Magnetic quantum dots for multimodal imaging. *Wiley Interdisciplinary Reviews. Nanomedicine and Nanobiotechnology*. 2009;**1**:475-491
- [88] Wang Y-XJ. Superparamagnetic iron oxide based MRI contrast agents: Current status of clinical application. *Quantitative Imaging in Medicine and Surgery*. 2011;**1**(1):35-40
- [89] Gao JH, Gu HW, Xu B. Multifunctional magnetic nanoparticles: Design, synthesis, and biomedical applications. *Accounts of Chemical Research*. 2009;**42**:1097-1107
- [90] Shi DL, Sadat ME, Dunn AW, Mast DB. Photo-fluorescent and magnetic properties of iron oxide nanoparticles for biomedical applications. *Nanoscale*. 2015;**7**:8209-8232
- [91] Bronzino JD, Peterson DR. *Biomedical Signals, Imaging, and Informatics*. Boca Raton: CRC Press, Taylor & Francis Group; 2015
- [92] Ahmed S, Dong J, Yui M, Kato T, Lee J, Park EY. *Journal of Nanobiotechnology*. 2013;**11**:28
- [93] Carretta P, Lascialfari A. *NMR-MRI, mSR and Mössbauer Spectroscopies in Molecular Magnets*. Springer-Verlag Mailand: Milan, Italy; 2007
- [94] Liu CH, Sahoo SL, Tsao MH. *Colloids and Surfaces. B, Biointerfaces*. 2014;**115**:150-156
- [95] Acharya A. Luminescent magnetic quantum dots for In vitro/ In vivo imaging and applications in therapeutics. *Journal of Nanoscience and Nanotechnology*. 2013;**13**:3753-3768
- [96] Zhang L, Wang Y, Tang Y, Jiao Z, Xie C, Zhang H, et al. High MRI performance fluorescent mesoporous silica-coated magnetic nanoparticles for tracking neural progenitor cells in an ischemic mouse model. *Nanoscale*. 2013;**5**:4506-4516
- [97] Catherine CB, Adam SGC. Functionalisation of magnetic

nanoparticles for applications in  
biomedicine. *Journal of Physics D:  
Applied Physics*. 2003;**36**:R198

[98] Gao G, Zhang Q, Yin T,  
Shapter JG, Lai W, Huang P, et al. *ACS  
Applied Materials & Interfaces*.  
2017;**9**:17777-17785

[99] Lu X, Jiang R, Fan Q, Zhang L,  
Zhang H, Yang M, et al. Fluorescent-  
magnetic poly(poly(ethyleneglycol)  
monomethacrylate)-grafted Fe<sub>3</sub>O<sub>4</sub>  
nanoparticles from post-atom-transfer-  
radical-polymerization modification:  
Synthesis, characterization, cellular  
uptake and imaging. *Journal of  
Materials Chemistry*. 2012;**22**:6965-6973